◆ Human Brain Mapping 22:83–96(2004) ◆

Comparison of Simultaneously Recorded [$H_2{}^{15}O$]-PET and LORETA During Cognitive and Pharmacological Activation

Alex Gamma,[1] Dietrich Lehmann,[2] Edi Frei,[1] Kazuki Iwata,[3] Roberto D. Pascual-Marqui,[2] and Franz X. Vollenweider[1]*

[1]*Research Unit, University Hospital of Psychiatry, Zurich, Switzerland*
[2]*The KEY-Institute for Brain-Mind Research, University Hospital of Psychiatry, Zurich, Switzerland*
[3]*Graduate School of Information Sciences, Tohoku University, Aoba-ku, Sendai, Japan*

Abstract: The complementary strengths and weaknesses of established functional brain imaging methods (high spatial, low temporal resolution) and EEG-based techniques (low spatial, high temporal resolution) make their combined use a promising avenue for studying brain processes at a more fine-grained level. However, this strategy requires a better understanding of the relationship between hemodynamic/metabolic and neuroelectric measures of brain activity. We investigated possible correspondences between cerebral blood flow (CBF) as measured by [H_2O]-PET and intracerebral electric activity computed by Low Resolution Brain Electromagnetic Tomography (LORETA) from scalp-recorded multichannel EEG in healthy human subjects during cognitive and pharmacological stimulation. The two imaging modalities were compared by descriptive, correlational, and variance analyses, the latter carried out using statistical parametric mapping (SPM99). Descriptive visual comparison showed a partial overlap between the sets of active brain regions detected by the two modalities. A number of exclusively positive correlations of neuroelectric activity with regional CBF were found across the whole EEG frequency range, including slow wave activity, the latter finding being in contrast to most previous studies conducted in patients. Analysis of variance revealed an extensive lack of statistically significant correspondences between brain activity changes as measured by PET vs. EEG-LORETA. In general, correspondences, to the extent they were found, were dependent on experimental condition, brain region, and EEG frequency. *Hum. Brain Mapp. 22:83–96, 2004.* © 2004 Wiley-Liss, Inc.

Key words: PET; CBF; LORETA; EEG; methodology

Contract grant sponsor: Swiss Federal Health Office (BAG); Contract grant number: 316.98.0686; Contract grant sponsor: Swiss National Science Foundation (SNF); Contract grant number: 31-52989.97; Contract grant sponsor: Heffter Research Institute, Santa Fe, NM; Contract grant number: HRI-CH02.2002; Contract grant sponsor: IGPP, Freiburg, Germany; Contract grant number: 670806.

*Correspondence to: Dr. Franz X. Vollenweider, PUK Zurich, Research Unit, Lenggstr. 31, 8029 Zurich, Switzerland.
E-mail: vollen@bli.unizh.ch

Received for publication 17 November 2003; Accepted 22 December 2003

DOI 10.1002/hbm.20015

INTRODUCTION

The established functional brain imaging methods such as Positron-Emission-Tomography (PET) and functional Magnetic Resonance Imaging (fMRI) are based on the detection of the hemodynamic or metabolic sequelae of neural activation. One strength of both methods is their high spatial resolution that, over the years, has been successfully driven into the low mm range. On the down side, PET in particular has poor temporal resolution in the range of 1 min for [$H_2{}^{15}O$]-PET and 30–45 min for [^{18}F]-Deoxyglucose-PET. Further, [H_2O]-PET is indirect insofar as it does not directly tap neuronal energy consumption but measures regional cerebral blood flow (rCBF), which is taken to be proportional to neuronal activity.

The disadvantages of CBF-PET are the advantages of the EEG: The EEG directly measures neuronal activity in terms of the electrical field produced by active neuronal populations (although it is not uniformly sensitive to all neural activity, favoring synchronous sources close to the scalp surface). Its temporal resolution is usually in the millisecond range, but can be arbitrarily high in theory and is in practice only limited by the sampling rate employed for data acquisition. Until recently, EEG has not been able to compute from the scalp-recorded voltages the intracerebral, three-dimensional configuration of the neural sources, without restricting the solution to a pre-selected (and typically, small) number of sources. The difficulty with this "inverse problem" is that there is no unique, non-ambiguous solution to it, i.e., there are infinitely many possible configurations of intracerebral neuroelectric generators that could have produced the electric field that is actually measured on the scalp. Thus, any algorithm that solves the inverse problem must necessarily be based on constraints imposed on the problem. One such algorithm that has gained particular attention recently is Low Resolution Brain Electromagnetic Tomography (LORETA) [Pascal-Marqui et al., 1994; Pascual-Marqui, 1999]. LORETA is based on the assumption that the "smoothest" distribution of neuroelectric generators is the most likely one, i.e., that the activity of neighboring neurons is maximally correlated [Llinás, 1988; Haalman and Vaadia, 1997]. Although LORETA has localization power [Pascual-Marqui, 1999], its spatial resolution is, unlike that of PET, very low (~3–4 cm).

Given their different strengths and shortcomings, the complementary use of PET/fMRI and EEG-LORETA is one of the most promising strategies to approach a methodical accuracy that will allow us to probe brain events at their own temporal and spatial scale. Its success, however, is dependent on an improved understanding of the relationship between these different indexes of brain activity. Only if we know *what* we measure, will we be able to integrate knowledge from different imaging modalities into a more comprehensive understanding of brain processes.

A number of previous studies have attempted to relate measures of spontaneous EEG activity to cerebral blood flow or metabolism [Buchsbaum et al., 1984; Guich et al., 1989; Günther et al., 1997; Ingvar et al., 1976; Melamed et al., 1975; Nagata et al., 1993; Obrist et al., 1963; Sulg et al., 1981; Szelies et al., 1999]. However, most of these studies have been conducted in psychiatric or neurologic patients whose brain functions and anatomy may be different in crucial ways from those of healthy subjects. Many early studies are further limited by using only very rough spatial measurements of brain activity (e.g., on the level of the whole brain or single hemispheres). Even those studies that used more fine-grained EEG and functional imaging measurements were facing the fundamental problem of having to relate *intracerebral* measures of blood flow or metabolism to *extracerebral* measures of brain electric activity.

This problem has been partly avoided in recent combined ERP and hemodynamic-based brain imaging studies [Heinze et al., 1998; Menon et al., 1997; Opitz et al., 1999]. Typically, these studies have fitted a small number of intracerebral equivalent dipoles to those brain regions where activation had previously been found in PET/fMRI using the same tasks and subjects. Although these studies have generally produced meaningful results, they are nevertheless not fit to answer questions about the correspondence of neuroelectric and hemodynamic measures, since they used the hemodynamic results to constrain neuroelectrical source localization, thus assuming an a priori correspondence between the two measures. Another drawback of this procedure is that whereas single dipole fitting may be adequate for localizing focal neural sources activated by sensory stimuli, it is generally unsuited for cognitive paradigms where multiple distributed loci of activation are likely. This latter case of distributed sources is adequately handled by LORETA, as reported in independent validations of LORETA's localization properties [review in Pascual-Marqui et al., 2002].

But one of the most serious limitations of previous multimodal imaging studies is the fact that measurements of the two modalities have not been made simultaneously. Although efforts were usually made to keep experimental setting and subjects constant, the interval between the measurements of the two modalities sometimes ranged up to several weeks. Thus, even if there was a one-to-one correspondence between neuroelectric and hemodynamic measures, considerable variance between non-simultaneous recordings could still be expected due to the fact that the same brain at two points in time will never be in identical states. Put differently, the very question of the degree of cross-modality correspondence can only be answered conclusively using simultaneous multi-modal measurement of one single brain. In the particular case of drug administration studies such as the present one, an added advantage of simultaneous recording is the fact that the number of drug administrations can be minimized. Also, sequential recordings would always raise concern whether the findings might not reflect or at least be confounded by habituation.

In attempting to avoid major limitations of earlier work, the present study aimed at clarifying the relationship between measures of brain activity obtained by [H_2O]-PET and EEG-LORETA. To this end, [H_2O]-PET and EEG were simul-

taneously recorded in 16 healthy subjects. Since previous studies indicated that the correspondence between imaging modalities is contingent upon experimental condition [e.g., Puce et al., 1995], we conducted our measurements during four conditions involving cognitive and pharmacological activation. EEG data were submitted to analysis with LORETA to assess the intracerebral distribution of neuroelectric activity. To maximize comparability between neuroelectric and hemodynamic measurements, the EEG signal was averaged over the 1-min period of PET acquisition. We thereby made the assumption that the most natural approach to establishing potential correspondences between the two methods was to operate them at the same temporal resolution, which in this case was dictated by the inherently low resolution of [H_2O]-PET. However, the high temporal resolution of EEG was still exploited for computing the FFT up to 30 Hz, which requires sampling points at least at about 16-msec intervals. The observed spatial patterns of brain activity during each condition as well as the differences between the conditions were visually and statistically compared on several levels. Importantly, the present analysis was done without prior hypotheses regarding the number, location, and/or strength of expected neural sources during any of the conditions.

SUBJECTS AND METHODS

Subjects

The study included 16 healthy volunteers (6 women, 10 men; mean age = 26.0 years, SD = 2.5 years), students recruited at the University of Zurich. At study entry, subjects were screened by psychiatric interview and somatic examinations including electrocardiogram, blood and urine analysis. Exclusion criteria were: major medical disorder, abnormal ECG, history of drug abuse, psychiatric disorder (either personal or in first-degree relatives), and pregnancy. All subjects gave their written consent after being informed by a written and oral description of the aim of the study, the procedures involved, and the effects and possible risks of MDMA administration. The study was carried out in accordance with the Declaration of Helsinki and approved by the Ethics Committee of the University Hospital of Psychiatry, Zurich.

Experimental Protocol

Subjects were examined during two pharmacological and two cognitive conditions. The pharmacological stimulation involved the administration of a single oral dose of 1.7 mg/kg 3,4-methylenedioxymethamphetamine (MDMA) or placebo in a double-blind, randomized, and counter-balanced fashion. The cognitive stimulation consisted (1) of the "A-X version" of the Continuous Performance Test (CPT) [Van Leeuwen et al., 1998] that requires the subject to keypress after the occurrence of the letter sequence A-X on the screen (the target), and (2) of an appropriate "control task," i.e., a stimulus condition that was identical to the CPT except that the target letters were omitted from the displayed stimulus material, and the subject was asked to merely observe the screen. Thus, each subject participated in a total of four conditions, given by the factorization of the two stimulation categories: Placebo/Control-Task, Placebo/CPT, MDMA/Control-Task, and MDMA/CPT. In each condition, the EEG and cerebral blood flow using [$H_2{}^{15}O$]-PET were simultaneously recorded for one minute.

EEG Measurements and Processing

The EEG was recorded from 31 electrodes that were applied according to the international 10/20 system (FP1/2, FPZ, F3/4, F7/8, FZ, FT9/10, FC5/6, T3/4, T5/6, TP9/10, C3/4, CZ, CP5/6, P3/4, PZ, PO9/10, O1/2, OZ). A further electrode was placed below the left eye to record eye movements. Both F3 and F4 served as common recording reference electrodes. The recordings were done using a 32-channel system (Neurofile System, Nihon Kohden), a sampling rate of 256 samples/sec and a 1–50 Hz bandpass filter. The EEG data were screened off-line for eye, muscle, movement, and technical artifacts. Two-second epochs of artifact free EEG were used for further analyses. If three or fewer EEG channels contained artifacts, they were interpolated, otherwise the epoch was rejected. If fewer than 10 sec of EEG within one recording session was acceptable, the subject was omitted from further analysis. After artifact screening, the EEG data from 10 subjects each in the Placebo-Control Task and MDMA-Control Task condition, 14 subjects in the Placebo-CPT condition, and 12 subjects in the MDMA-CPT condition were available for further analysis. Regarding the paired comparisons, 9 subjects were available for the comparison between placebo and MDMA during the control task, and 12 during the CPT, while 10 subjects were available for the comparison between the control task and the CPT during placebo, and 7 during MDMA. On the average across subjects, 31.9 sec of data (range: 14–46 sec) for the Placebo/Control-Task condition, 32.5 sec (22–64 sec) for the Placebo/CPT condition, 22.2 sec (14–46 sec) for the MDMA/Control-Task condition, and 23.5 sec (10–48 sec) for the MDMA/CPT condition were available for analysis. Spatial DC offset was removed (average reference recomputation). Since EEG spectral frequency bands reflect different functions and behave statistically independently, further analysis was performed separately in the following seven bands [Kubicki et al., 1979]: Delta (1.5–6 Hz), Theta (6.5–8 Hz), Alpha1 (8.5–10 Hz), Alpha2 (10.5–12 Hz), Beta1 (12.5–18 Hz), Beta2 (18.5–21 Hz), and Beta3 (21.5–30 Hz). All epochs were submitted to FFT. For each condition, frequency band, and electrode position, mean power was computed and averaged across subjects.

LORETA

LORETA was used to compute the intracortical distribution of the electric activity from the surface EEG data [Pascal-Marqui et al., 1994; Pascual-Marqui, 1999]. LORETA computes current density at each voxel in the solution space as the linear, weighted sum of the scalp electric potentials

[Pascual-Marqui, 1995]. It solves the inverse problem based on the assumption that the smoothest of all possible activity distributions is the most plausible one. This assumption is supported by electrophysiology, where neighboring neuronal populations show highly correlated activity [Haalman and Vaadia, 1997; Llinás, 1988]. Thus, EEG-LORETA results in solutions where neighboring voxels have maximally similar activity. Regardless of the electrophysiological validity of the smoothness constraint, LORETA has been shown to be capable of correct 3-D localization, although with blurring, i.e., low resolution [Pascual-Marqui, 1999].

The utilized version of LORETA employed a three-shell spherical head model registered to the Talairach human brain atlas [Talairach and Tournoux, 1988] available as digitized MRI from the Brain Imaging Center, Montreal Neurologic Institute. The registration between spherical and Talairach head geometry used the realistic EEG electrode coordinates reported by Towle et al. [1993]. The LORETA solution space was restricted to the cortical gray matter and hippocampus in the Talairach atlas as defined by the corresponding digitized Probability Atlas available from the Brain Imaging Center, Montreal Neurologic Institute. A total of 2,394 voxels at 7-mm spatial resolution were produced under this neuroanatomical constraint. There was one 3-D LORETA image for each subject for each condition and frequency band. These images will be called "raw activity images." Details on the use of LORETA to compute generators of EEG frequency components can be found in Frei et al. [2001].

PET

[$H_2{}^{15}O$]-PET scans were performed on a General Electric Advance PET scanner in 3-D-acquisition mode. For each subject and condition, two 1-min scans were obtained, and cerebral blood flow (CBF) was measured as the accumulated counts during scan time. Mean doses of 400–500 MBq radioactivity per scan were administered through an indwelling catheder. The resulting images were processed using the statistical parametric mapping software (SPM99). Individual scans were realigned, normalized to the same Talairach coordinate system as the LORETA images (the "MN305" brain), and smoothed with a gaussian filter of 15 mm FWHM [Friston et al., 1996]. The resulting images will be called "raw activity images."

Comparison between CBF-PET and EEG-LORETA

The present data was subjected to five levels of analysis. On each level, a comparison was made between PET and EEG-LORETA. For the 5 levels this comparison included:

1. Raw activity images for each condition
2. Correlations between raw activity images for each condition
3. Unfiltered t-images showing differences between pairs of conditions
4. Brain areas showing statistically significant differences between pairs of conditions
5. Correlations between images of differences between pairs of conditions

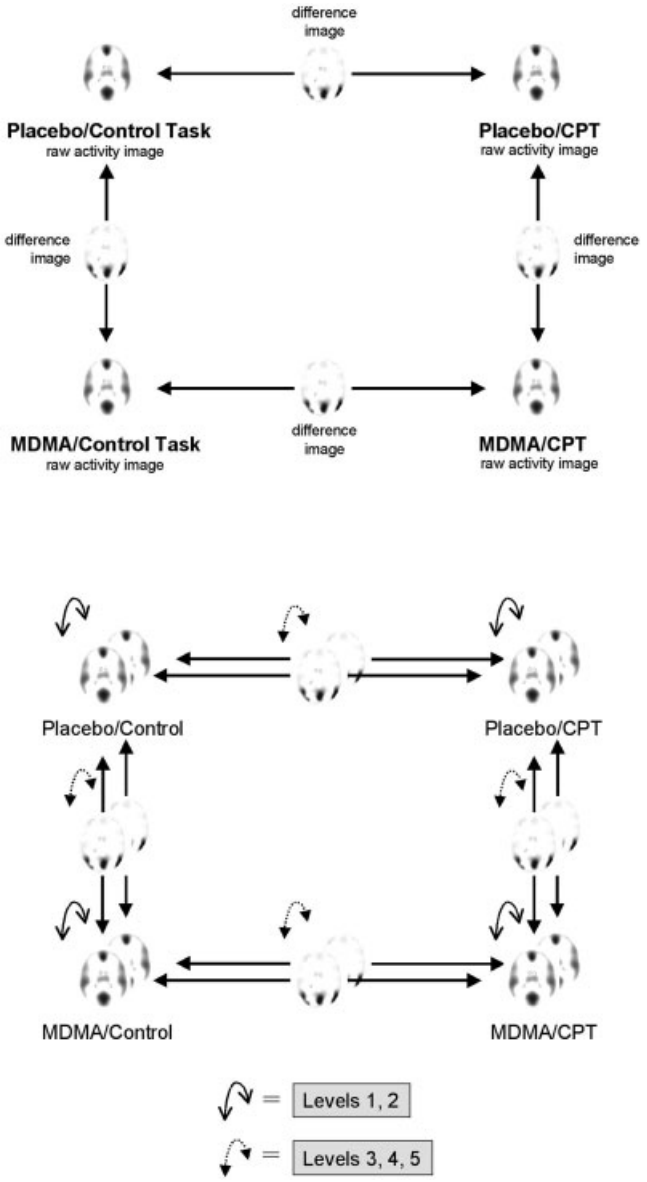

Figure 1.
Top: Comparisons between conditions performed within each imaging modality separately (PET and LORETA). **Bottom:** The different levels of analysis to compare results across imaging modalities (PET vs. LORETA, shown as superposed layers). Levels 1 and 2: comparison of raw images; levels 3–5: comparison of differences images. See text for further explanation.

These different levels of analysis are graphically depicted in Figure 1.

Level 1: Raw Activity Images

Images of raw activity for each condition were visually compared between PET and EEG-LORETA. The lower end of the activity spectrum was removed from the images by compressing the color scale by 75%. This procedure left only a number of separate, clearly identifiable blobs of peak brain activity to be easily compared across image modalities. The purpose of this analysis was to allow for a rough, qualitative overview of the extent to which CBF and electric brain activity may coincide.

Level 2: Correlations Between Raw Activity Images

Correlations between PET and EEG-LORETA raw activity images were computed for each condition. This procedure included the computation of Pearson's correlation coefficients for each corresponding pair of voxels over the entire brain volume. The resulting correlation images were thresholded at a level that corresponded to a statistically significant correlation at $P < 0.05$ for the number of subjects available for the respective condition (this threshold was close to $r = 0.6$ for all conditions). In order to enhance the detection of patterns of correlations, no correction for multiple testing was applied.

Level 3: Unfiltered t-Images of Differences Between Conditions

For each PET and EEG-LORETA, statistical differences between pairs of conditions as shown in Figure 1, were computed as images of t-values. For PET, the t-statistic was computed using statistical parametric mapping (SPM99) and an ANOVA design with proportional scaling used to control for variance in global activity. For LORETA, a pseudo t-statistic was computed, as previously described [Frei et al., 2001], using a non-parametric randomization approach as proposed by Holmes et al. [1996]. The pseudo t-statistic was based on images of log-transformed power normalized to a common global activity level, which has a similar effect as the proportional scaling procedure applied to the PET images. Thus, similar relative measures of activity were used for PET and LORETA. Neither PET nor EEG-LORETA t-images were thresholded, in order to allow the visual detection of patterns of similarity that may lie or extend below levels of statistical significance.

Level 4: Images of Statistically Significant Differences Between Conditions

On this level of analysis, the t-images were assessed for statistical significance. For PET, statistical inferences were based on an ANOVA model using proportional scaling of the data to adjust for differences in global activity levels, and were corrected for multiple testing. For statistical inference in LORETA, the randomized pseudo t-images were thresholded at the conventional 5% probability level. For both methods, inferences were based on single voxel intensities ("voxel statistics") and spatial extent ("cluster statistics"). PET and EEG-LORETA images of relative activity were then visually compared for correspondences in both location and direction of brain activity changes.

Level 5: Correlations Between Difference Images

Pearson's correlations between PET and EEG-LORETA difference images were computed for each of the four pairs of difference between conditions. Again, voxel-by-voxel correlation coefficients were computed and the resulting correlations were thresholded at a statistical level of significance of $P < 0.05$ (uncorrected for multiple comparisons).

Note that since PET and EEG-LORETA produce incommensurable measures of brain activity, a direct statistical or quantitative comparison between the two imaging modalities is not possible for the analyses in levels 1, 3, and 4. Only the correlation analyses of levels 2 and 5 can be quantitative.

Substance

Racemic MDMA (3, 4-methylenedioxymethamphetamine) was obtained through the Swiss Federal Health Office (BAG), Department of Pharmacology and Narcotics, Bern, from EPROVA AG, Schaffhausen, and prepared as capsules (10 and 50 mg) at the Pharmacy of the Kantonsspital, Luzern, Switzerland. The use of MDMA was approved by the Swiss Federal Health Office, Berne.

RESULTS

Level 1: Raw Activity Images

Figure 2 shows PET and EEG-LORETA raw activity images for the Placebo/Control-Task condition. In PET, areas of peak CBF were the medial frontal, anterior and posterior cingulate, parietal, temporal and medial occipital cortices, and the thalamus (which does not belong to the solution space of LORETA). EEG-LORETA showed peak electrical activity in the medial and lateral occipital cortex in all frequency bands. Beta2 and β3 contained additional peak activity in the medial and lateral frontal cortex and the anterior cingulate, which was not evident in the alpha bands and less so in the delta, theta, and β1 bands. The β3 band, and less so β2, also contained bilateral temporal activity peaks. In comparison, activity measured by PET and EEG-LORETA overlapped in the medial prefrontal cortex, the anterior cingulate, medial occipital, and bilateral temporal cortex. Activity unique to PET was revealed in the posterior cingulate and parietal cortex. Activity unique to EEG-LORETA was found in lateral occipital cortex. The results were basically identical in the other three conditions (not shown).

Level 2: Correlations Between Raw Activity Images

Images of correlations between raw activity as measured by PET vs. EEG-LORETA were available for all four conditions: Placebo/Control-Task, Placebo/CPT, MDMA/Control-Task, and MDMA/CPT.

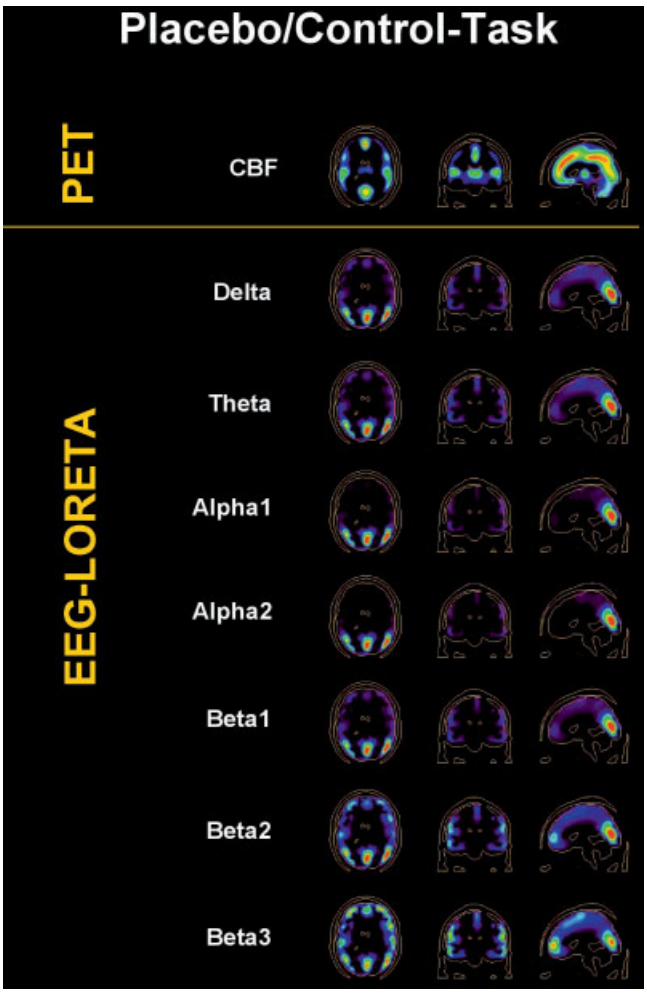

Figure 2.
Brain activity during the control task after administration of a placebo, shown in transverse, coronal, and sagittal view. **Top row:** CBF as measured by [H_2O]-PET. **Following rows:** Neuroelectric activity as computed by LORETA for seven frequency bands. Brighter hues indicate stronger activity. Images are sliced at z = 22 mm (transverse), y = −26 mm (coronal), and x = 0 mm (sagittal), with the coordinate origin located at the anterior commissure.

Placebo/Control-Task (Fig. 3). In this condition, only positive correlations between CBF and brain electric activity were present. The most extensive correlations were observed in the beta bands, where areas of correlation included the bilateral fronto-temporal cortices, the central frontal and cingulate cortices, the subgenual cortex, and the right posterior temporal cortex in the β3 band. Correlations in the theta and alpha bands were evident in the left and right frontal cortex.

Placebo/CPT: No significant correlations were present in this condition.

MDMA/Control-Task (Fig. 3): Again, only positive correlations were present and were most pronounced in the β2 and β3 bands. These bands showed extensive correlations involving the occipital and parietal cortices. The delta and theta bands showed correlations in the anterior cingulate. An additional area of correlation in the delta band was seen in the right temporal cortex.

MDMA/CPT: No significant correlations were present in this condition.

In summary, only positive correlations between CBF as measured by [H_2O]-PET and neuroelectric activity as measured by EEG-LORETA were found. No correlations were present in those conditions that involved cognitive stimulation by a Continuous Performance Test.

Since there might be concern about the relatively short duration of the analyzed EEG data, the data analysis of this level 2 was re-done, doubling the minimal required period of usable EEG to 20 sec. This increased the length of the available EEG to 27–37 sec, depending on the experimental condition. On the whole, the results were very similar to those with the 10-sec requirement; they showed the same complete lack of negative correlations for all four conditions. Regarding positive correlations, the results for two of the four conditions (Placebo-Control Task and Placebo-CPT) were nearly identical. The results of the MDMA-CPT condition were similar, but α2 and β3 showed central frontal correlations where previously there were none. In the MDMA-Control condition, positive correlations for α2 and β1 differed from the original results, while those for delta and theta were similar but more extensive. Beta2 and β3 showed virtually identical correlations. In conclusion, although there are some differences to the original analysis, these do not have a major impact on the results and their interpretation.

Level 3: Unfiltered t-Images of Differences Between Conditions

Four sets of t-images were available for each PET and EEG-LORETA, corresponding to the four pairs of differences between conditions: Placebo/Control-Task minus MDMA/Control-Task, Placebo/CPT minus MDMA/CPT, Placebo/Control-Task minus Placebo/CPT, and MDMA/Control-Task minus MDMA/CPT. The first two pairs reveal drug-related differences, the latter two pairs reveal task-related differences in brain activity.

Placebo-Control-Task minus MDMA/Control-Task (Fig. 4): The PET image showed a striking uniform decrease in CBF over the whole brain volume during MDMA compared to placebo. A similar extensive deactivation was evident in the EEG-LORETA images for the theta and α1 band. The delta band showed a weak left-sided decrease, paired with a right temporo-occipital increase in electrical activity. The α2 band showed extensive decreases and increases restricted to the left fronto-temporal cortex. The beta bands were dominated by increased anterior and posterior activity and negligible decreases.

Placebo-CPT minus MDMA/CPT: Again, the PET image showed a global uniform decrease in CBF during MDMA. In EEG-LORETA, slow wave activity in the delta and theta bands was largely decreased with the exception of

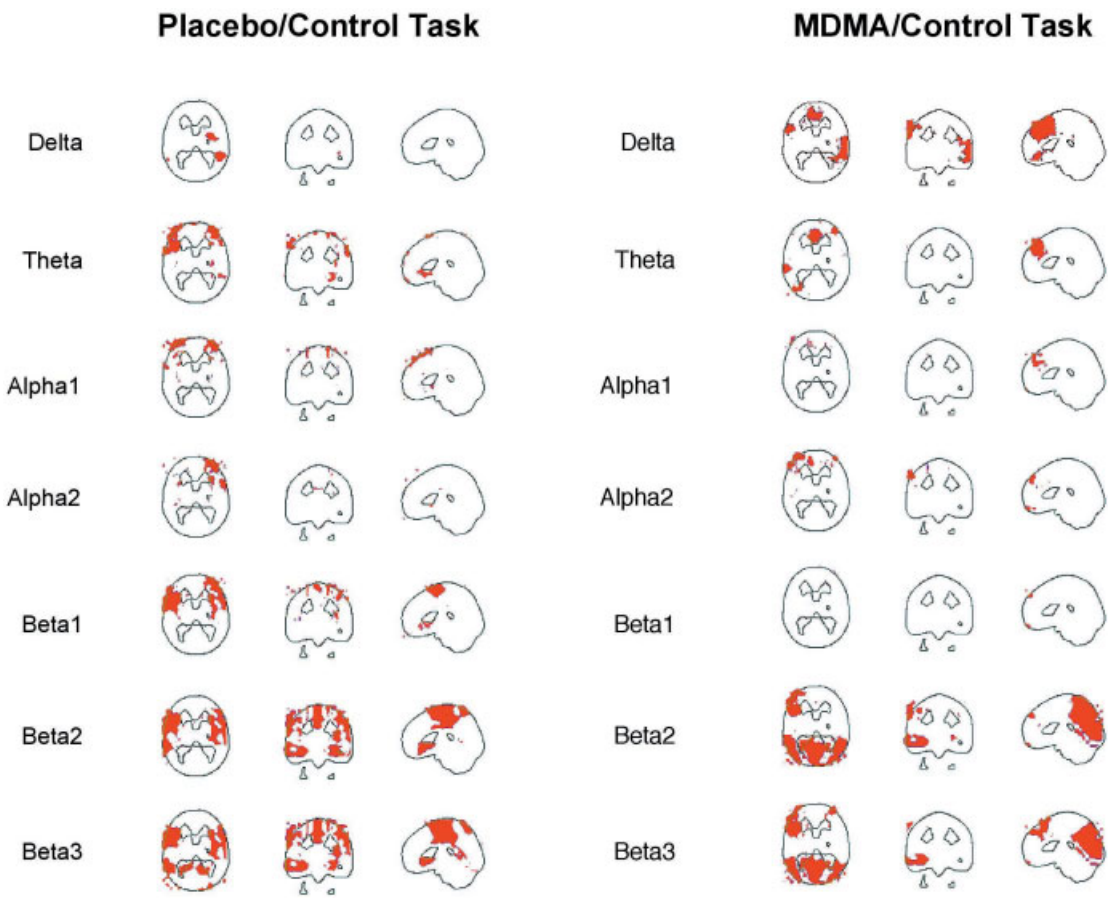

Figure 3.

Correlations between CBF and neuroelectric activity in the different frequency bands during the control task under placebo (**left**) and MDMA (**right**). Positive correlations above the significance threshold of r = 0.6 are shown in red. No negative correlations emerge. Except for the delta band, images are sliced at z = 22 mm (transverse), y = −26 mm (coronal), and x = 0 mm (sagittal), with the coordinate origin located at the anterior commissure. The delta band transverse views are sliced at z = −14 mm in order to better show the regions of correlations.

weak temporal and occipital increases. The α bands were characterized by ventral frontal and temporal increases and posterior decreases. The beta bands were dominated by pronounced frontal and occipital increases, with decreases confined to the cingulate cortex. Thus, the pattern of a global unidirectional change as evident in the PET image was not reflected in any EEG frequency band.

Placebo/Control-Task minus Placebo/CPT (Fig. 4): The PET image showed a rather complex pattern of CBF changes, with CPT-related increases mainly in the occipital and left ventral prefrontal cortex, and a marked decrease in the right temporal cortex, and less pronounced decreases in the left temporal and dorsal frontal cortex. In EEG-LORETA, activity changes in the delta band were small, with some increases in dorsal frontal and occipital cortex. The theta band was dominated by global activation. Both alpha and beta bands showed increased activity in the anterior brain, and decreased activity in posterior regions.

MDMA/Control-Task minus MDMA/CPT: The CPT-related pattern of changes of CBF was similar to the previous one. Increases dominated in the occipital and frontal cortices, and decreases were strongest in the right posterior temporal, and less so in the left temporal cortex. Interestingly, a similar, although smaller, "cold spot" of peak decreases in the right posterior temporal cortex was seen in the EEG-LORETA images of the delta, α1, β1, and β3 bands. Otherwise, the delta band showed weak changes dominated by a strip of deactivation in the parietal and posterior cingulate cortex. Large, but weak increases and decreases in medial central cortex were seen in the theta band. The α1 band showed weak occipital and medial parietal decreases and right fronto-temporal increases in electrical activity. In contrast, α2 was weakly, but uniformly activated. All beta bands were similar in showing left fronto-temporal and medial central activation (including the cingulate cortex) and right-sided temporo-occipital deactivation, which extended to fronto-

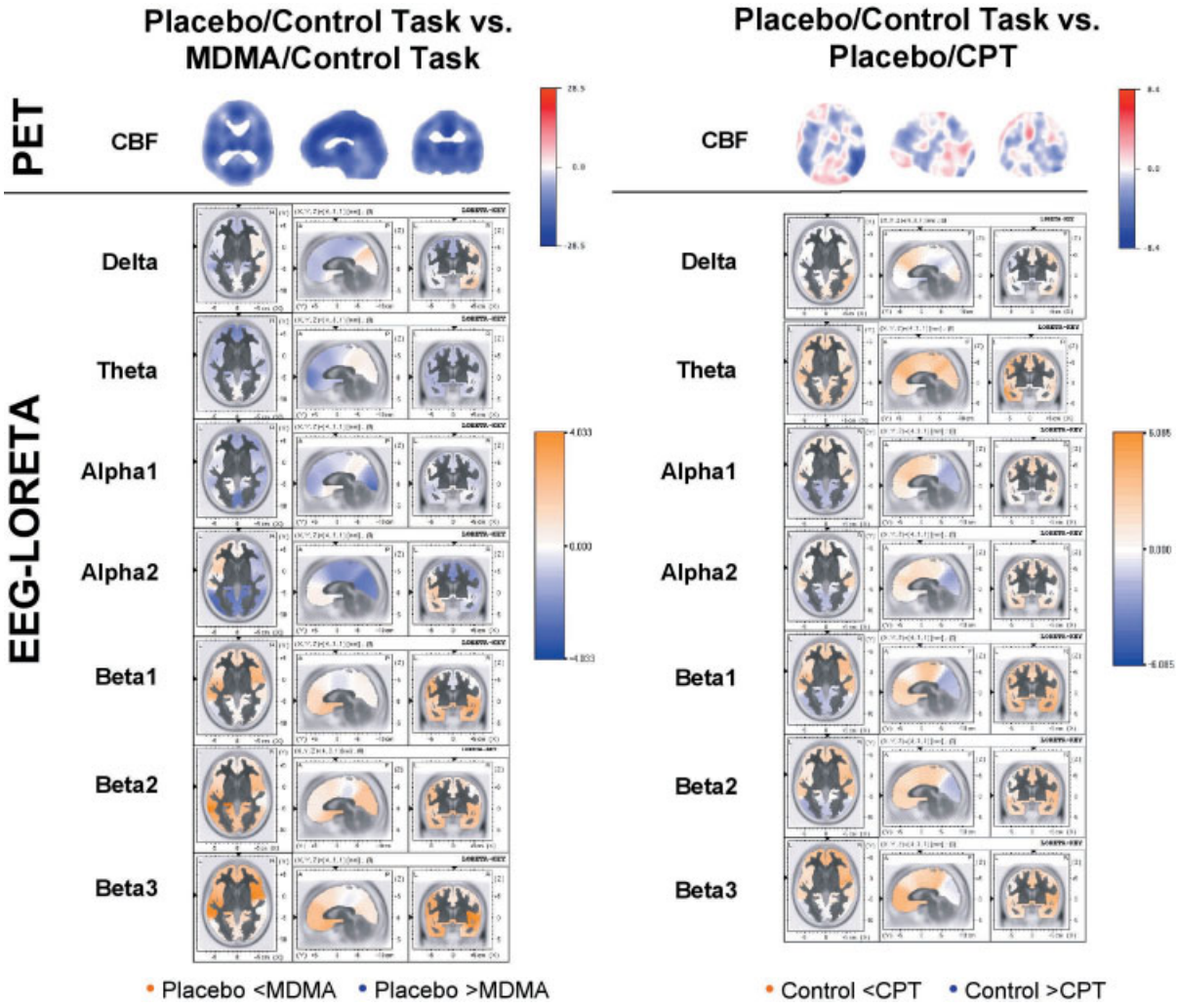

Figure 4.

Color-coded images showing the differences between placebo and MDMA during the control task (**left**) and the difference between the control task and the CPT during placebo (**right**), expressed as t-value distribution. Orange of increasing intensity indicates increasing positive t-values, blue of increasing intensity indicates increasing negative t-values. **Top rows:** CBF as measured by PET. **Following rows:** Neuroelectric activity as computed by LORETA. The LORETA t-images of different frequency bands are scaled to a common maximum to make them directly comparable. PET images are sliced at z = 22 mm (transverse), y = −26 mm (coronal), and x = 0 mm (sagittal), with the coordinate origin located at the anterior commissure. LORETA images are sliced at the anterior commissure.

temporal regions in the β2 and β3 bands. The overall pattern of changes seen in PET was not mirrored in any EEG frequency band.

Level 4: Images of Statistically Significant Differences Between Conditions

When comparing PET with EEG-LORETA results, we will only consider overlapping activity changes of similar size, which may indicate a specific correspondence between PET and EEG-LORETA activity changes. We do not attempt to give a strict definition of the "similar size" criterion, since such strictness seems premature at this point and might unnecessarily obscure the detection of potentially important correspondences. We also report overlapping changes in opposite directions, since it may well be that an increase in CBF corresponds to a decrease in electrical activity in some frequency range and vice versa.

In general, although many changes in brain activity could be observed in both imaging modalities, there were very few correspondences between the modalities that were region-specific. Table I lists, for each of the four comparisons between conditions, the cortical brain regions that showed

TABLE I. Brain areas of statistically significant change between pairs of experimental conditions for both PET and LORETA

	PET						LORETA			
Region	*x*	*y*	*z*	*P*	Region	Band	*x*	*y*	*z*	*P*
Placebo/control task vs. MDMA/control task										
Plac < MDMA										
L Orbitofrontal (B11)	−18	26	−16	0.05	Whole brain, except central frontal, posterior cingulate, mediodorsal prefrontal	β2				0.02[a]
R Occipital (B31)	20	−72	28	0.009	Whole brain, except central frontal, posterior cingulate, parietal, left temporoo-ccipital, right fusiform	β3				0.03[a]
L Inferior occipital (B18)	−20	−84	−8	0.05						
L Occipital (B17)	−12	−88	4	0.05						
Plac > MDMA										
R Insula (B13)	50	10	4	0.001	L Parietal supramarginal (B40)	β3				0.03[a]
L Amygdala/L Cingulate (B34)	−14	−2	−12	0.03						
R Paracentral lobule (B31)	2	−26	44	0.004						
Anterior cingulate (B24)	0	2	32	0.004						
L Anterior cingulate (B24)	−4	8	28	0.006						
R Anterior cingulate (B32)	4	8	40	0.006						
Posterior cingulate (B31)	**0**	**−28**	**36**	**0.007**	**Posterior Cingulate (B31/23)**	**β2**				**0.02[a]**
R Superior frontal (B6)	10	−12	−64	0.05						
R Anterior cingulate (B24)	2	−8	36	0.05						
Placebo/CPT vs. MDMA/CPT										
Plac < MDMA										
L Inferior occipital (B18)	**−20**	**−82**	**−8**	**0.004**	**L Inferior occipital (B18/19)**	**β3**	**−38**	**−38**	**−13**	**0.05[b]**
					L Prefrontal, L temporal, occipital	β3				0.006[a]
R Anterior cingulate (B32)	16	38	−4	0.001	L Ventrolateral prefrontal, R orbitofrontal, R anterior temporal, R dorsomedial prefrontal, anterior cingulate	α2				0.01[a]
R Medial frontal (B10)	8	62	0	0.02						
L Fusiform gyrus	−44	−8	−24	0.02						
Plac > MDMA										
R paracentral lobule (B31)	2	−20	44	0.001	Temporal, occipital, central frontal, cingulate	α2				0.01[a]
Medial frontal (B6)	0	−8	52	0.001	L Posterior superior temporal (B39)	α2	−52	−60	29	0.05[b]
R Anterior cingulate (B24)	4	−2	44	0.001						
L Anterior superior temporal (B22)	−50	−2	4	0.001						
R Anterior superior temporal (B22)	52	0	4	0.001						
Placebo/control task vs. Placebo/CPT										
Control < CPT										
L Orbitofrontal (B11)	−40	36	−22	0.001	R Inferior parietal (B40)	Δ	60	−46	43	0.05[b]
L Dorsoventral prefrontal (B10)	−28	62	−6	0.001	R Inferior parietal (B40)	Δ				0.012[a]
L Superior occipital (B19)	**−30**	**−82**	**24**	**0.03**	L Medial temporal (B21)	θ	−59	−4	−20	0.05[b]
					Whole brain, except L fusiform, L temporo-occipital	θ				0.002[a]
L Occipital (B17/18)	−2	−90	2	0.04	Temporal, frontal	β1				0.001[a]
L Pre-/postcentral	−44	−22	62	0.05	R Prefrontal, central frontal, cingulate, R temporal, L inferior temporal	β2				0.031[a]
					R Insula	β3	39	−11	1	0.05[b]
					Medial prefrontal, R temporal, R insula, posterior cingulate	β3				0.01[a]
Control > CPT										
L Medial frontal (B11)	−22	36	−8	0.002	L Precuneus, L fusiform	θ				0.002[a]
L Inferior frontal (B9)	−32	18	28	0.001	Posterior cingulate, occipital	β1				0.001[a]
L Medial front (B46)	−32	18	18	0.001	**L Occipital**	**β2**				**0.031[a]**
R Inferior frontal (B45)	56	16	6	0.001						
R Frontal (B8)	18	14	42	0.004						
R Precentral B44	52	12	12	0.004						
R Anterior cingulate (B24)	16	6	44	0.004						
R Medidal frontal (B6)	12	−2	58	0.001						
L Insula (B13)	−34	22	8	0.001						
R Anterior superior temporal (B22)	58	10	−2	0.001						
MDMA/control task vs. MDMA/CPT										
Control < CPT					(no significant changes)					
R Dorsomedial prefrontal (B10)	14	68	8	0.05						
L Anterior cingulate (B32)	−14	30	18	0.05						
L Superior frontal (B9)	−14	46	34	0.05						
L Medial occipital (B18/19)	−30	−86	10	0.001						
Control > CPT					(no significant changes)					
R temporal pole (B36)	26	−6	−32	0.001						
R Medial temporal (B39)	46	−72	14	0.001						
R Transveral temporal (B41)	48	−26	14	0.007						
R Superior temporal (B22)	54	−24	2	0.007						
R Insula (B13)	44	−26	22	0.007						

[a] Cluster statistics; [b] voxel statistics (see Methods section).
Areas in boldface within sections indicate changes in PET and LORETA in corresponding brain areas of similar size, either in uniform or opposite direction. Note that Talairach coordinates cannot be given for LORETA results based on cluster statistics.

significant changes in rCBF (PET) and neuroelectric activity (EEG-LORETA). The only specific regional correspondences between PET and EEG-LORETA activity changes were found for the beta frequency band. During the control task, both CBF and neuroelectric activity in the β2 band were decreased by MDMA in the posterior cingulate (Brodman

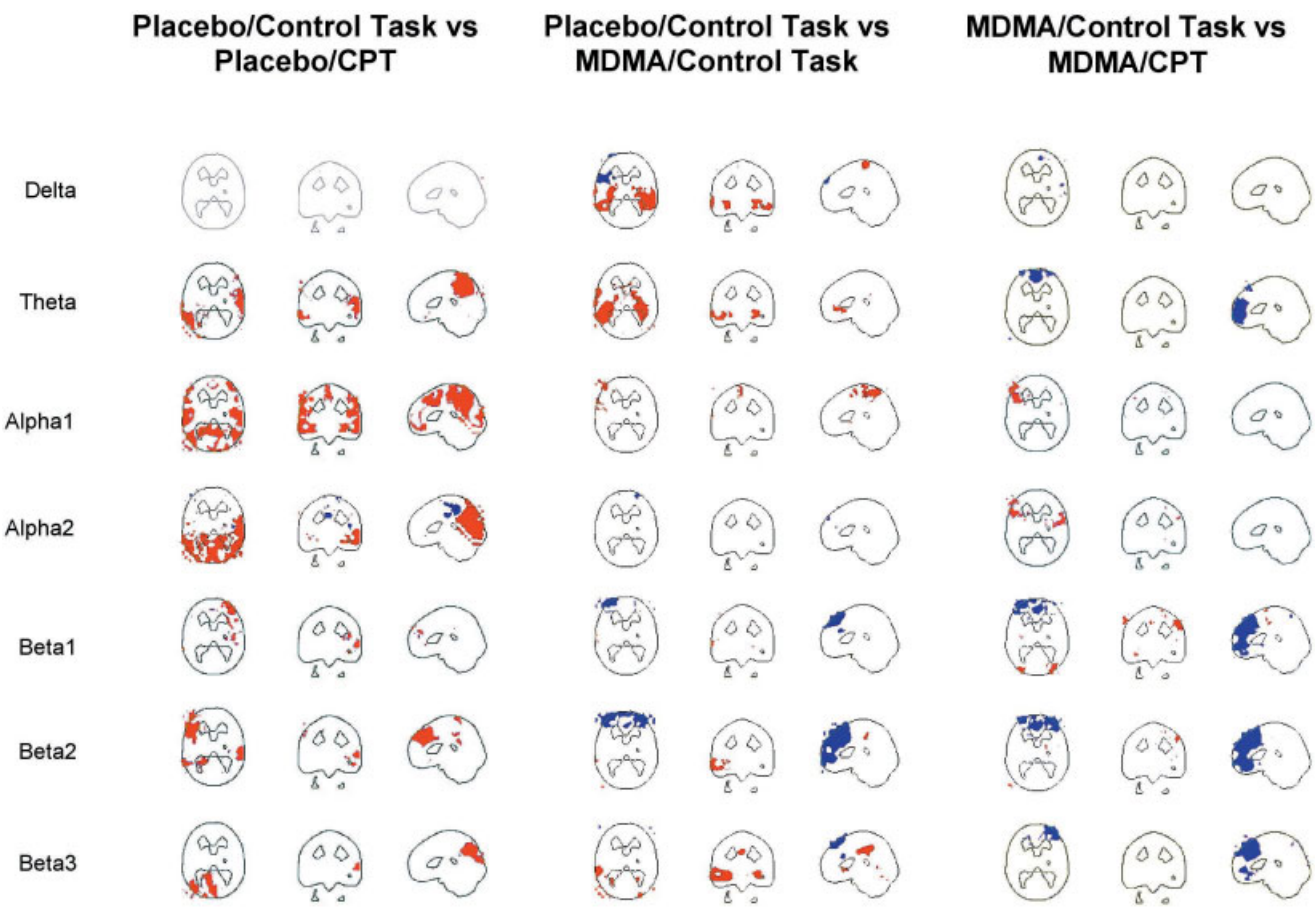

Figure 5.

PET-LORETA correlations between images of difference between the control task and the CPT during placebo (**left**), between placebo and MDMA during the control-task (**middle**), and between control task and the CPT during MDMA (**right**). Red colors indicate positive, blue colors indicate negative supra-threshold correlations ($r \geq |0.6|$). Images are sliced at z = 22 mm (transverse), y = −26mm (coronal), and x = 0 mm (sagittal), with the coordinate origin located at the anterior commissure. The transvers delta and theta band images in the middle display are sliced at z = − 8 mm to better show regions of correlations.

area 31) compared to placebo. During the CPT, there was a common MDMA-induced increase in CBF and electric activity in the β3 band in the left inferior occipital cortex (Brodman area 18). Finally, during placebo, the CPT increased CBF, but decreased neuroelectric activity in the beta2 band in the left occipital cortex. No other overlaps of comparable extent were observed.

Level 5: Correlations Between Difference Images

Placebo/Control-Task Minus MDMA/Control-Task (Fig. 5): Similar positive correlations were found for the delta and theta frequency range, including mainly the bilateral posterior temporal cortex. A negative correlation was found in the delta band in the left dorsolateral prefrontal cortex. Negative correlations were also dominant in the β1/2 frequency range in the dorsal prefrontal cortex. In the β3 band, this negative correlation was still present in a small area of dorsal prefrontal cortex, but additional positive correlations in the left temporal cortex were observed.

Placebo/CPT Minus MDMA/CPT: Strikingly, the only result found was a negative correlation in the right dorsal frontal cortex in the α2 band.

Placebo/Control-Task minus Placebo/CPT (Fig. 5): Positive correlations were clearly dominant in this comparison. No correlations were present in the delta band. The theta band showed positive correlations in the medial and left parietal cortex, the left temporo-occipital and right temporal cortex. Both the α1 and α2 band showed extensive bilateral positive correlations in the parietal and occipital cortex. In the α1 band, the area of correlation extended to the (bilateral) dorsal frontal cortex. Beta2 was dominated by a positive correlation in the medial and left dorsolateral prefrontal cortex, while β3 showed a positive correlation in the medial and left parieto-occipital cortex.

MDMA/Control-Task Minus MDMA/CPT (Fig. 5): Interestingly, negative correlations dominated this comparison. Again, no correlation was found in the delta band. A negative correlation in the medial prefrontal cortex was seen in the theta band. The α bands showed some small positive correlations in the left dorsolateral prefrontal cortex. Extensive areas of negative correlation were found in the prefrontal cortex and anterior cingulate in the beta frequency range.

DISCUSSION

This study compared measurements of brain activity recorded simultaneously by [H_2O]-PET and EEG-LORETA, using different levels of analysis. Comparing raw activity between PET and EEG-LORETA in four different conditions, we found both overlapping as well as modality-specific, unique regions of brain activity. This indicates, unsurprisingly, that there may be no one-to-one correspondence between CBF and neuroelectric activity. A quantified assessement of the relationship between CBF and neuroelectric activity using correlation analysis showed localized positive correlations between CBF and electric activity in the delta, theta, and beta frequency bands. The positive relationship observed in the beta band is consistent with results from previous studies, and is in the expected direction given the common interpretation of beta as excitatory activity. The positive correlation of CBF with theta activity in the anterior cingulate is consistent with a similiar correlation of theta activity with glucose consumption in a combined FDG-PET/EEG-LORETA study [Pizzagalli et al., 2003]. The positive relationship of CBF with delta band activity, however, is in the opposite direction to many earlier combined EEG and hemodynamic/metabolic studies, which have contributed to the interpretation of delta as inhibitory activity. Part of the explanation for this discrepancy may be that the large majority of these studies have been conducted in neurologic patients [Nagata, 1988; Szelies et al., 1999; Valladares-Neto et al., 1995], whose functional neuroanatomy may be severely abnormal. In fact, the few studies in normal subjects show correlations in opposite directions to those in patients [Rainville et al., 1999] or an entire lack of correlations [Buchan et al., 1997; Obrist et al., 1963]. It has been suggested that this lack of correlations might be due to small variability in normal brain activity, preventing the detection of possible correlations. This explanation has some plausibility in the case of delta activity, which is largely absent during relaxed wakefulness in healthy adults.

Our data, however, do not support a general lack of correspondence between slow wave activity and CBF in normals. Rather, they demonstrate that correspondences are present but do not generally coincide with those found in patients. This may indicate that delta activity plays a different role in the normal compared to the pathological brain. There is evidence that delta activity in normal subjects is not exclusively inhibitory, as it has been associated with attention to internal processing and reaction time during mental tasks. In addition, hemodynamic changes as measured by PET and fMRI might not only reflect excitatory but also inhibitory activity, resulting in positive correlations between EEG delta and hemodynamic/metabolic activity even if delta were largely inhibitory.

Interestingly, no significant correlations were present in the two conditions involving the CPT task, suggesting that cognitive activation by the CPT may uncouple CBF from neuroelectric activity or that there is too little variance in brain activity during the CPT for any correlations to emerge. Comparing the PET/EEG-LORETA correlations between the other two conditions (involving the control task) revealed that, although correlations were in the same direction, they were largely found in different brain areas. The general conclusion is that correlations between PET and EEG-LORETA are both task- and region-dependent.

Considering the t-images of difference between pairs of conditions, it is evident that within each imaging modality, the two images of differences across tasks (for both drug conditions) and the two images of difference across drugs (for both task conditions) are very similar. Comparing t-images across imaging modalities, however, revealed little in the way of PET/EEG-LORETA correspondences that would be consistent across the four different comparisons between pairs of conditions. Even within a given comparison between a pair of conditions, neuroelectric activity changes in a given frequency band and brain region sometimes were in the same direction as CBF changes, whereas they were in the opposite direction in another brain region in the same frequency band. A limited PET/EEG-LORETA correspondence may hold for the two comparisons across drug conditions. Here, a striking global decrease of CBF was matched by similarly widespread (though not completely global) decreases in the slow wave and α bands and increases in the beta bands. This correspondence did not hold, however, for the two comparisons across task conditions. Again, the conclusion is that PET/EEG-LORETA correspondences, as far as they exist, are dependent on task, region, and frequency band. A similar point emerges from the comparison of the images of statistically significant differences between pairs of conditions: the very few PET/EEG-LORETA correspondences that were present did not generalize across different pairs of conditions.

The quantitative assessment of correlations between changes in CBF and neuroelectric activity further supports the notion of task-, region-, and frequency-dependence of PET/EEG-LORETA correspondences. Beta band changes correlated positively or negatively with CBF changes, depending on the comparison and brain region examined. Alpha and theta changes correlated positively with CBF changes in only one of the four comparisons (Placebo/Control-Task vs. Placebo/CPT). Similarly, delta and theta changes correlated positively with CBF changes in only one comparison (Placebo/Control-Task vs. MDMA/Control-Task). The lack of PET/EEG-LORETA correlations in the comparison involving the two CPT conditions (Placebo/CPT vs. MDMA/CPT) may reflect the lack of PET/EEG-LORETA correlations within each of the two conditions.

One major strength of the present study compared to most previous work is the simultaneous multi-modal recording. Simultaneous recording is the only way to ensure that measurement modalities tap one and the same brain state, and is thus a prerequisite for a conclusive answer to the question of cross-modality correspondence. One difficulty arises when considering that simultaneous recording is obviously much easier to achieve for combined EEG/PET studies than for combined EEG/fMRI studies because of the gross interference in EEG data from the MRI scanner. The latter co-recordings, however, are preferable since fMRI has superior temporal resolution in the range of one to several seconds. The necessary methodology presently becomes available [e.g., Allen et al., 2000; Lemieux et al., 2001].

A second strength of this study is the use of an intracranial measure of neuroelectric activity, based on the LORETA algorithm. Apart from limiting the solution space to the cortex and hippocampus, LORETA makes no a priori assumptions about the number and location of neuroelectrical sources, thus producing source configurations that are more realistic, in particular for cognitive studies. Very recently, Vitacco et al. [2002] have used LORETA to address the issue of cross-modality correspondence in a combined ERP/fMRI study using a complex visual language task. Although measurements of the two modalities were separated by 1 to 3 weeks, they found reasonable agreement in terms of the distance between peak activations detected by the two modalities (average distance 14.5 mm). The match was significant in half of the ten subjects, indicating a lack of strict one-to-one correspondence. The part of the present analysis most comparable with the analysis used by Vitacco et al. [2002] is the comparison between the statistically significant changes produced by EEG-LORETA and PET (analysis level 4). Here it would seem that the results from Vitacco and colleagues show much stronger correspondence between neuroelectric and hemodynamic signals than our study, as evidenced by the almost complete lack of common significant cross-modal activations found in our study. Upon closer examination, however, it becomes evident that apart from the use of LORETA, the two studies are difficult to compare. We used [H_2O]-PET whilst Vitacco et al. [2002] used fMRI, which may have a different signal-to-noise ratio. We temporally integrated brain signals over one minute, whereas Vitacco et al. averaged only over half a second of data. Our analysis was based on EEG signals not time-locked to stimulus onset, while time-locked ERPs were used by Vitacco et al. [2002]. Relative to EEG signals, ERPs have different spatial, temporal, and spectral characteristics that may lead to different detectability on the scalp. Finally, we used a simple attentional task whereas Vitacco et al. [2002] used a more complex semantic decision task.

In this context, the general question arises to what extent the observed relative paucity of cross-modal correspondence is due to a genuine lack of correspondence between measures of neuroelectric and hemodynamic brain activity or to methodological shortcomings of our study. Concerning the latter possibility, it may be that our methods to compare EEG and PET have been inadequate, or that temporal data integration over one minute involving inter-individual variation in duration and sampling of EEG epochs may have obscured real cross-modal correspondences that might have been evident at a finer time scale. The fact that LORETA has very low spatial resolution, in part due to the use of ony 31 electrodes, further limits the potential correspondences detectable by our approach. Regarding the different levels of analysis, the correlation analyses are the most direct way of comparing modalities and, therefore, probably most reliable in revealing true cross-modality correspondences. The comparison of SPM-type statistical inferences across modalities involves more intervening steps of data processing and may introduce sources of divergence that are not present in the original data. But there are also many inherent differences between neuroelectric and hemodynamic measures (as also suggested by EEG-fMRI comparisons) [e.g., Laufs et al., 2003] and thus there are many conceivable instances where the two measures may diverge. In general, the two measures may have different signal-to-noise ratios, and thus different sensitivities to real activations. Specific circumstances may produce an EEG/ERP signal without hemodynamic signature (e.g., brief, transient neural events, or changes in oscillatory or spectral properties without net hemodynamic changes), or a hemodynamic signal without EEG/ERP signature (e.g., deep electric sources, cancellation of electric sources, or increases in non-synchronous neural activity).

CONCLUSION

To the extent that EEG-LORETA has been and continues to be validated as correctly localizing cortical neuroelectric activity [see, e.g., Lavric et al., 2001; Pizzagalli et al., 2000; Steger et al., 2001; Thut et al., 2000; Waberski et al., 2001; Winterer et al., 2001], our present findings show extensive positive correlations of CBF with high-frequency beta activity, more circumscribed positive correlations with slow wave delta and theta activity, and little correlation with medium-frequency α activity in normal subjects during cognitive non-engagement. These correlations were lost, however, during a state of cognitive activation, indicating either uncoupling or reduced variability of CBF and neuroelectric activity. There were almost no common significant peak changes in the two imaging modalities as revealed by statistical parametric mapping. In general, correspondences found between PET and EEG-LORETA measurements in normal subjects were task/condition-, frequency-, and region-dependent. These multiple dependencies indicate that there are no generally applicable rules of thumb connecting measures of brain electric activity with cerebral blood flow.

ACKNOWLEDGMENTS

This work was supported in part by the Heffter Research Institute, Santa Fe, NM (HRI-CH02.2002 to F.X.V.) and by IGPP, Freiburg, Germany (670806 to D.L.).

REFERENCES

Allen PJ, Josephs O, Turner R (2000): A method for removing imaging artifact from continuous EEG recorded during functional MRI. Neuroimage 12:230–239.

Buchan RJ, Nagata K, Yokoyama E, Langman P, Yuya H, Hirata Y, Hatazawa J, Kanno I (1997): Regional correlations between the EEG and oxygen metabolism in dementia of Alzheimer's type. Electroencephalogr Clin Neurophysiol 103:409–417.

Buchsbaum MS, Kessler R, King A, Johnson J, Cappelletti J (1984): Simultaneous cerebral glucography with positron emission tomography and topographic electroencephalography. In: Pfurtscheller G, Jonkman EJ, Lopes da Silva FH, editors. Brain ischemia : quantitative EEG and imaging techniques. Amsterdam: Elsevier Science Publishers B.V. p. 263–269.

Frei E, Gamma A, Pascual-Marqui RD, Lehmann D, Hell D, Vollenweider FX (2001): Localization of MDMA-induced brain activity in healthy volunteers using low resolution brain electromagnetic tomography (LORETA). Hum Brain Mapping 14:152–165.

Friston KJ, Ashburner J, Frith CD, Poline JB, Heather JD, Frackowiak RJS (1996): Spatial registration and normalization of images. Hum Brain Mapping 2:165–189.

Guich SM, Buchsbaum MS, Burgwald L, Wu J, Haier R, Asarnow R, Nuechterlein K, Potkin S (1989): Effect of attention on frontal distribution of delta activity and cerebral metabolic rate in schizophrenia. Schizophr Res 2:439–448.

Günther W, Müller N, Knesewitsch P, Haag C, Trapp W, Banquet J-P, Stieg C, Alper KR (1997): Functional EEG mapping and SPECT in detoxified male alcoholics. Eur Arch Psychiatry Clin Neurosci 247:128–136.

Haalman I and Vaadia E (1997): Dynamics of neuronal interactions: relation to behavior, firing rates, and distance between neurons. Hum Brain Mapping 5:249–253.

Heinze HJ, Hinrichs H, Scholz M, Burchert W, Mangun GR (1998): Neural mechanisms of global and local processing: a combined PET and ERP study. J Cognit Neurosci 10:485–498.

Holmes AP, Blair RC, Watson JDG, Ford I (1996): Nonparametric analysis of statistic images from functional mapping experiments. J Cereb Blood Flow Metab 16:7–22.

Ingvar DH, Sjölund B, Ardö A (1976): Correlation between dominant EEG frequency, cerebral oxygen uptake and blood flow. Electroencephalogr Clin Neurophysiol 41:268–276.

Kubicki S, Herrmann WM, Fichte K, Freund G (1979): Reflections on the topics: EEG frequency bands and regulation of vigilance. Pharmakopsychiatr Neuropsychopharmakol 12:237–245.

Laufs H, Kleinschmidt A, Beyerle A, Eger E, Salek-Haddadi A, Preibisch C, Krakow K (2003): EEG-correlated fMRI of human alpha activity. Neuroimage 19:1463–1476.

Lavric A, Pizzagalli D, Forstmeier S, Rippon G (2001): A double-dissociations of English past-tense production revealed by event-related potentials and low-resolution electromagnetic tomography (LORETA). Clin Neurophysiol 12:1833–1849.

Lemieux L, Salek-Haddadi A, Josephs O, Allen P, Toms N, Scott C, Krakow K, Turner R, Fish DR (2001): Event-related fMRI with simultaneous and continuous EEG: Description of the method an initial case report. Neuroimage 14:780–787.

Llinás RR (1988): The intrinsic electrophysiological porperties of mammalian neurons: insights into central nervous system function. Science 242:1654–1664.

Melamed E, Lavy S, Portnoy Z, Sadan S, Carmon A (1975): Correlation between regional cerebral blood flow and EEG frequency in the contralateral hemisphere in acute cerebral infarction. J Neurol Sci 26:21–27.

Menon V, Ford JM, Lim KO, Glover GH, Pfefferbaum A (1997): Combined event-related fMRI and EEG evidence for temporal-parietal cortex activation during target detection. Neuroreport 8:3029–3037.

Nagata K (1988): Topographic EEG in brain ischemia: correlation with blood flow and metabolism. Brain Topogr 1:97–106.

Nagata K, Yuya H, Nara M, Kondoh Y, Watahiki Y, Satoh Y, Hirata Y, Hatazawa J (1993): Thyrotropin-releasing hormone (TRH) enhances correlations between EEG and cortical blood flow and metabolism in spinocerebellar degeneration. Electroencephalogr Clin Neurophysiol 2:S1–S148.

Obrist WD, Sokoloff L, Lassen NA, Lane MH, Butler RN, Feinberg I (1963): Relation of EEG to cerebral blood flow and metabolism in old age. Electroencephalogr Clin Neurophysiol 15:610–619.

Opitz B, Mecklinger A, Von Cramon DY, Kruggel F (1999): Combining electrophysiological and hemodynamic measures of the auditory oddball. Psychophysiology 36:142–147.

Pascual-Marqui RD (1995): Source localization: continuing discussion of the inverse problem. ISBET Newslett 6:9–30.

Pascual-Marqui RD (1999): Review of methods for solving the EEG inverse problem. Int J Bioelectromagn 1:75–86.

Pascal-Marqui RD, Michel CM, Lehmann D (1994): Low resolution electromagnetic tomography: a new method for localizing electrical activity in the brain. Int J Psychophysiol 18:49–65.

Pascual-Marqui RD, Esslen M, Kochi K, Lehmann D (2002): Functional imaging with low resolution brain electromagnetic tomography (LORETA): a review. Method Find Exp Clin 24C: 91–95.

Pizzagalli D, Lehmann D, Koenig T, Regard M, Pascal-Marqui RD (2000): Face-elicited ERPs and affective attitude: brain electric microstate and tomography analyses. Clin Neurophysiol 111: 521–531.

Pizzagalli D, Oakes T, Davidson J (2003): Coupling of theta activity and glucose metabolism in the human rostral cingulate cortex: an EEG/PET study of normal and depressed subjects. Psychophysiology 40:939–949.

Puce A, Constable TC, Luby ME, McCarthy G, Nobre AC, Spencer DD, Gore JC, Allison T (1995): Functional magnetic resonance imaging of sensory and motor cortex: correlation with electrophysiological methods. J Neurosurg 83:270.

Rainville P, Hofbauer RK, Paus T, Duncan GH, Bushnell MC, Price DD (1999): Cerebral mechanisms of hypnotic induction and suggestion. J Cognit Neurosci 11:110–125.

Steger J, Imhof K, Denoth J, Pascal-Marqui RD, Steinhausen H-C, Brandeis D (2001): Brain mapping of bilateral visual interactions in children. Psychophysiology 38:243–253.

Sulg IA, Sotaniemi KA, Tolonen U, Hokkanen E (1981): Dependence between cerebral metabolism and blood flow as reflected in the quantitative EEG. A clinical review. Adv Biol Psychiat 6:102–108.

Szelies B, Mielke R, Kessler J, Heiss W-D (1999): EEG power changes are related to regional cerebral glucose metabolism in vascular dementia. Electroencephalogr Clin Neurophysiol 110:615–620.

Talairach J, Tournoux P (1988): Co-planar stereotaxic atlas of the human brain. Stuttgart: Thieme.

Thut G, Hauert CA, Viviani P, Morand S, Spinelli L, Blanke O, Landis T, Michel C (2000): Internally driven vs. externally cued movement selection: a study on the timing of brain activity. Cognit Brain Res 9:261–269.

Towle VL, Bolanos J, Suarez D, Tan K, Grzeszczuk R, Levin DN, Cakmur R, Frank SA, Spire JP (1993): The spatial location of EEG electrodes: locating the best-fitting sphere relative to cortical anatomy. Electroencephalogr Clin Neurophysiol 86:1–6.

Valladares-Neto DC, Buchsbaum MS, Evans WJ, Nguyen D, Nguyen P, Siegel BV, Stanley J, Starr A, Guich S, Rice D (1995): EEG delta, positron emission tomography, and memory deficit in alzheimer's disease. Neuropsychobiology 31:173–181.

Van Leeuwen TH, Brandeis D, Overtoom KE, Pascual-Marqui RD, Van't Klooster B, Rothenberger A, Sergeant JA, Steinhausen H-C (1998): The continuous performance test revisited with neuroelectric brain mapping: impaired orienting in children with attention deficits. Behav Brain Res 94:97–110.

Vitacco D, Brandeis D, Pascal-Marqui RD, Martin E (2002): Correspondence of event-related potential tomography and functional magnetic resonance imaging during language processing. Hum Brain Mapping 17:4–12.

Waberski TD, Kreitschmann-Andermahr I, Kawohl W, Darvas F, Ryang Y, Gobbele R, Buchner H (2001): Spatio-temporal source imaging reveals subcomponents of the human auditory mismatch negativity in the cingulum and right inferior temporal gyrus. Neurosci Lett 308:107–110.

Winterer G, Mulert C, Mientus S, Gallinat J, Schlattmann P, Dorn H, Herrmann WM (2001): P300 and LORETA: Comparison of normal subjects and schizophrenic patients. Brain Topogr 13:299–313.